Medium/high-field magnetoconductance in chaotic quantum dots

2001 J. Phys.: Condens. Matter 13 2935

(http://iopscience.iop.org/0953-8984/13/13/307)

INSTITUTE OF PHYSICS PUBLISHING JOURNAL OF PHYSICS: CONDENSED MATTER

J. Phys.: Condens. Matter **13** (2001) 2935–2945 www.iop.org/Journals/cm PII: S0953-8984(01)17672-1

Medium/high-field magnetoconductance in chaotic quantum dots

E Louis[1] **and J A Vergés**[2]

[1] Departamento de Física Aplicada and Unidad Asociada of the Consejo Superior de Investigaciones Científicas, Universidad de Alicante, Apartado 99, E-03080 Alicante, Spain
[2] Instituto de Ciencia de Materiales de Madrid, Consejo Superior de Investigaciones Científicas, Cantoblanco, E-28049 Madrid, Spain

Received 3 October 2000, in final form 25 January 2001

Abstract

The magnetoconductance G in chaotic quantum dots at medium/high magnetic fluxes Φ is calculated by means of a tight-binding Hamiltonian on a square lattice. Chaotic dots are simulated by introducing diagonal disorder on surface sites of $L \times L$ clusters. It is shown that when the ratio W/L is sufficiently large, W being the width of the leads, G increases steadily (almost with no fluctuations) showing a maximum at a magnetic flux $\Phi_{\max} \propto L^2/W$ (a flux at which the cyclotron radius $r_c \approx W/2$). Neither regular nor bulk disordered ballistic cavities (with a content of impurities proportional to L) show this effect. On the other hand, for magnetic fluxes such that $r_c > L/2$ and up to the aforementioned maximum, the average magnetoconductance increases almost linearly with the flux with a slope proportional to W^2. These results closely follow a theory proposed by Beenakker and van Houten to explain the magnetoconductance of two point contacts in series.

1. Introduction

Magnetoconductance in chaotic quantum dots has attracted a great deal of attention in recent years [1–4]. Weak-localization effects have been thoroughly investigated, with differences between chaotic and regular cavities being searched for [1, 3]. More recently, the self-similar character of magnetoconductance fluctuations in chaotic quantum dots has warranted several experimental studies [2, 4]. In reference [4] it was reported that in cavities with sufficiently soft walls, rather wide leads and a high zero-field conductance of the order of 40 conductance quanta, fluctuations were very weak and the magnetoconductance increased steadily by approximately 20% over 50 flux quanta [4]. Although an increase in the magnetoconductance as a function of the magnetic flux in cavities with wide leads may not be that surprising, no theoretical analysis of this result is yet available. This is so despite the wealth of experimental and theoretical information on magnetoconductance in related mesoscopic systems [5–10].

The purpose of the present work is to investigate the magnetoconductance of chaotic quantum dots over a wide range of magnetic field. Quantum dots are described by means of

0953-8984/01/132935+11$30.00

a tight-binding Hamiltonian on $L \times L$ clusters of the square lattice. Non-regular (chaotic) behaviour is induced by introducing disorder at surface sites, a procedure that has been shown to reproduce all properties of quantum chaotic cavities [11]. The most outstanding conclusions derived from our study are the following. For sufficiently open systems, large lead width W or, alternatively, high zero-field conductance, the magnetoconductance increases steadily as a function of the magnetic flux, reaching a maximum at a magnetic flux $\Phi_{\max}$ proportional to L^2/W, W being the width of the leads. This effect, which is in agreement with experimental observations [4], does not show up in regular or bulk disordered cavities. The average magnetoconductance versus magnetic flux curve shows four clearly differentiated regions:

(i) At small fluxes (typically below 1–2 flux quanta) the weak-localization peak with the typical Lorentzian shape is observed.
(ii) This is followed by a flux range over which the magnetoconductance shows a non-universal behaviour which depends on the configuration of the leads.
(iii) The latter lasts until the cyclotron radius becomes of the order of $L/2$. Beyond this point the average magnetoconductance increases linearly with the magnetic flux with a slope which increases with the square of the width of the leads (for very small W the slope is nearly zero and the magnetoconductance remains constant over a large flux range).
(iv) At large fluxes (cyclotron radii larger than $W/2$) the magnetoconductance decreases stepwise (each step of one flux quantum), due to the successive crossings of the Fermi energy of the transverse modes that contribute to the current.

As discussed below, these results are compatible with a theory proposed by Beenakker and van Houten [10] to interpret the experimental results for the magnetoconductance of two point contacts in series [9].

The rest of the paper is organized as follows. Section 2 includes a description of our model of a chaotic quantum dot and of the method that we used to compute the current. The results are presented in section 3, and discussed in terms of the theory of reference [10]. Section 4 is devoted to summarizing the conclusions of our work.

2. Model and methods

2.1. Model

The quantum dot is described by means of a tight-binding Hamiltonian with a single atomic level per lattice site on $L \times L$ clusters of the square lattice:

$$\widehat{H} = \sum_{m,n\in \mathrm{IS}} \omega_{m,n} |m,n\rangle\langle m,n| - \sum_{\langle m,n;m',n'\rangle} t_{m,n;m',n'} |m,n\rangle\langle m',n'| \tag{1}$$

where $|m,n\rangle$ represents an atomic orbital on site (m,n). Indices run from 1 to L, and the symbol $\langle\ \rangle$ denotes that the sum is restricted to nearest neighbours. Using Landau's gauge, the hopping integral is given by

$$t_{m,n;m',n'} = \begin{cases} \exp\left(2\pi \mathrm{i} \dfrac{m}{(L-1)^2}\Phi\right) & m = m' \\ 1 & \text{otherwise} \end{cases} \tag{2}$$

where the magnetic flux Φ is measured in units of the quantum of magnetic flux $\Phi_0 = h/e$. The energy $\omega_{m,n}$ of atomic levels at impurity sites (IS) is randomly chosen between $-\Delta/2$ and $\Delta/2$, whereas at other sites, $\omega_{m,n} = 0$. Impurities were taken on all surface sites [11, 13] except those coinciding with the lead entrance sites to avoid excessive (unphysical) scattering.

This model has been proposed to simulate cavities with rough boundaries and its properties closely follow those characterizing quantum chaotic systems [11,13]. Some calculations were also carried out on clusters with $2L$ bulk impurities[1].

2.2. Conductance

The conductance (measured in units of the quantum of conductance $G_0 = e^2/h$) was computed by using an efficient implementation of the Kubo formula. The method is described in [14], while applications to mesoscopic systems can be found in [15,16]. For a current propagating in the x-direction, the static electrical conductivity is given by

$$G = -2\left(\frac{e^2}{h}\right) \mathrm{Tr}[(\hbar\hat{v}_x)\,\mathrm{Im}\,\widehat{\mathcal{G}}(E)(\hbar\hat{v}_x)\,\mathrm{Im}\,\widehat{\mathcal{G}}(E)] \tag{3}$$

where $\mathrm{Im}\,\widehat{\mathcal{G}}(E)$ is obtained from the advanced and retarded Green functions:

$$\mathrm{Im}\,\widehat{\mathcal{G}}(E) = \frac{1}{2\mathrm{i}}[\widehat{\mathcal{G}}^R(E) - \widehat{\mathcal{G}}^A(E)] \tag{4}$$

and the velocity (current) operator $\hat{v}_x$ is related to the position operator $\hat{x}$ through the equation of motion $\hbar\hat{v}_x = [\widehat{H}, \hat{x}]$, $\widehat{H}$ being the Hamiltonian.

Numerical calculations were carried out connecting quantum dots to semi-infinite leads of width W in the range 1–L. The hopping integral inside the leads and between the leads and the dot at the contact sites is taken equal to that in the quantum dot (ballistic case). Assuming the validity of both the one-electron approximation and linear response, the exact form of the electric field does not change the value of G. An abrupt potential drop at one of the two junctions provides the simplest numerical implementation of the Kubo formula [14] since, in this case, the velocity operator has finite matrix elements for only two adjacent layers and Green functions are just needed for this restricted subset of sites. Assuming this potential drop to occur on the left-contact (lc) side, the velocity operator can be explicitly written as

$$\mathrm{i}\hbar v_x = -\sum_{j=1}^{W}(|\mathrm{lc},\, j\rangle\langle 1,\, j| - |1,\, j\rangle\langle \mathrm{lc},\, j|) \tag{5}$$

where $(|\mathrm{lc},\, j\rangle$ are the atomic orbitals at the left-contact sites that are nearest neighbours to the dot.

The Green functions are given by

$$[E\widehat{I} - \widehat{H} - \widehat{\Sigma}_1(E) - \widehat{\Sigma}_2(E)]\widehat{\mathcal{G}}(E) = \widehat{I} \tag{6}$$

where $\widehat{\Sigma}_{1,2}(E)$ are the self-energies introduced by the two semi-infinite leads [6]. Most calculations were carried out by assuming that the magnetic field was zero outside the dot. Under this assumption the retarded self-energy due to the mode of the wavevector k_y can be calculated explicitly:

$$\Sigma(E) = \frac{1}{2}\big(E - \epsilon(k_y) - \mathrm{i}\sqrt{4 - (E - \epsilon(k_y))^2}\big) \tag{7}$$

for energies within its band $|E - \epsilon(k_y)| < 2$, where $\epsilon(k_y) = 2\cos(k_y)$ is the eigenenergy of the mode k_y which is quantized as $k_y = (n_{k_y}\pi)/(W+1)$, n_{k_y} being an integer in the range from 1 to W. The transformation from the normal modes to the local tight-binding basis is obtained from the amplitudes of the normal modes, $\langle n|k_y\rangle = \sqrt{2/(W+1)}\sin(nk_y)$. Some calculations were done taking the magnetic field on the leads equal to that within the dot. For such cases

[1] This model has been shown to follow the characteristics of quantum chaotic systems [17]. The key point is that chaotic behaviour is obtained whenever the number of impurities is proportional to L.

the self-energy was calculated by iterating Dyson's equation. If not specified, calculations discussed hereafter correspond to the case of no magnetic field in the leads. Calculations were carried out on clusters of linear size $L = 47$–394 (in units of the lattice constant), with a fixed, arbitrarily chosen, Fermi energy, $E = -\pi/3$, and a disorder parameter $\Delta = 6$ [11]. In some cases, averages over disorder realizations were also taken. Although most calculations were performed with input/output leads of width W connected from site $(1, 1)$ to site $(1, 1 + W)$, and from (L, L) to $(L, L - W)$, respectively, other input/output lead configurations were also explored. All calculations on disordered systems were made at a fixed value of the disorder parameter, $\Delta = 6$.

3. Results

We first discuss results for a ratio W/L similar to that used in the experiments of reference [4]. In that work, conductance measurements were taken on a stadium cavity with a lithographic radius of 1.1 μm and leads 0.7 μm wide, which gives a ratio W/L of 0.64. Figure 1 shows the results for the magnetoconductance in cavities of linear sizes in the range $L = 47$–394 and leads of width $W = 0.65L$. The results correspond to a single realization of disorder. The most interesting result is the steady increase of the conductance with the magnetic field. The conductance reaches a maximum at a magnetic flux $\Phi_{\max}$ which, as illustrated in the inset of the figure, increases linearly with the linear size of the system L. At higher fields it decreases stepwise (visible lower right in figure 1; see also below). The increase in G before the maximum is reached can be as high as 30%. Note that, as the results of figure 1 correspond to $W \propto L$, they do not allow one to derive the actual relation between $\Phi_{\max}$ and the dimensional parameters W and L. The results discussed below show, however, that $\Phi_{\max} \propto L^2/W$. It is interesting to note that the increase in the conductance occurs with rather weak fluctuations

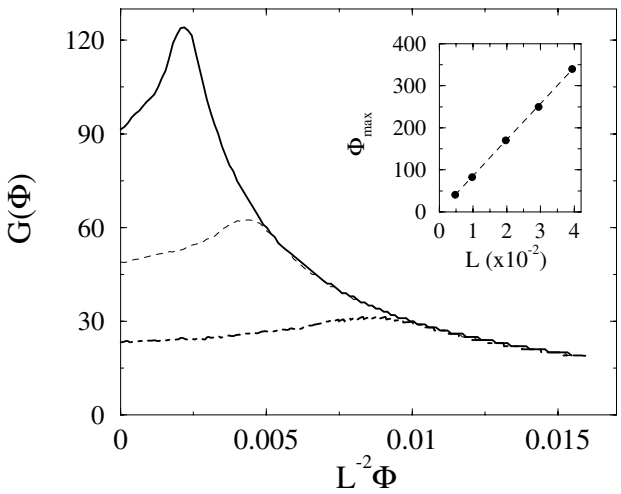

Figure 1. Magnetoconductance versus magnetic flux multiplied by the inverse of the dot area (both in units of their respective quanta), in dots of linear size L and leads of width W (connected at opposite corners) with a similar W/L ratio of $\approx$0.65. Results for $(L, W) = (97, 63)$, chain line, (197, 127), broken line, and (394, 254), continuous line, are shown. The results correspond to a single realization of disorder (Anderson impurities at surface sites with $\Delta = 6$) and a Fermi energy $E = -\pi/3$. Inset: the flux at which the magnetoconductance is maximum is plotted as a function of the linear size of the dot L. The fitted straight line is $\Phi_{max}/\Phi_0 = 0.026 + 0.86L$.

due to the large W/L ratio (or degree of opening) of the cavity (see [16]). Although the experimental data were taken at fields not high enough for observing the maximum shown in figure 1, it can be safely assumed that our results are compatible with those of reference [4].

Including the magnetic field in the leads does not change qualitatively the results discussed above. Figure 2 shows the magnetoconductance for cavities of linear size $L = 97$ with leads of width $W = 63$, and a single realization of disorder. The two calculations (with or without field in the leads) give very similar results for fluxes up to $\Phi \approx 30$, and differ only at a quantitative level at larger fluxes. A possible reason for the similarity between the two calculations is that, as the Green function of the whole system is calculated through Dyson's equation (see equation (6)), the region of the leads close to the dot is distorted by the magnetic field even in the case where no magnetic field is explicitly included in the leads. This result has an important consequence: as from an experimental point of view neither of the two calculations is realistic (the leads will probably be partially located within the non-zero-field region), the fact that these two limiting calculations give very similar results allows one to carry either of the two rather confidently.

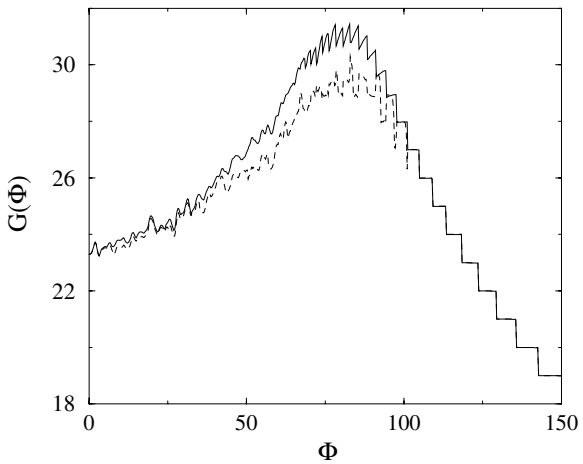

Figure 2. Magnetoconductance versus magnetic flux (both in units of their respective quanta), in dots of linear size $L = 97$ and leads of width $W = 63$ (connected at opposite corners of the dot). The results correspond to a single realization of disorder (Anderson impurities at surface sites with $\Delta = 6$), a Fermi energy $E = -\pi/3$, and systems with (broken line) or without (continuous line) magnetic field in the leads.

In figure 3 we compare the results for the cavity with surface disorder with those for a regular cavity and for a cavity with $2L$ bulk impurities. The results indicate that the cavity having surface disorder is the only one that reproduces the experimental results [4]. In regular cavities the conductance does not increase steadily due to the large-amplitude oscillation discussed in [16]. This behaviour clearly differentiates regular and chaotic cavities. At large fields the result for the cavity with surface disorder coincides with that for the regular cavity. This is a consequence of the fact that for sufficiently high fields the current is dominated by edge-like states which are not affected by surface disorder. Semiclassically, one can view carrier motion as short orbits bouncing off the same boundary. The associated quantum states have chirality and are thus commonly referred to as chiral states or edge states. The stepwise decrease of the magnetoconductance observed in regular and chaotic cavities with surface disorder is a consequence of the overall depopulation of Landau levels. It is interesting to note that the cavity with bulk disorder shows a markedly different behaviour, as this type of

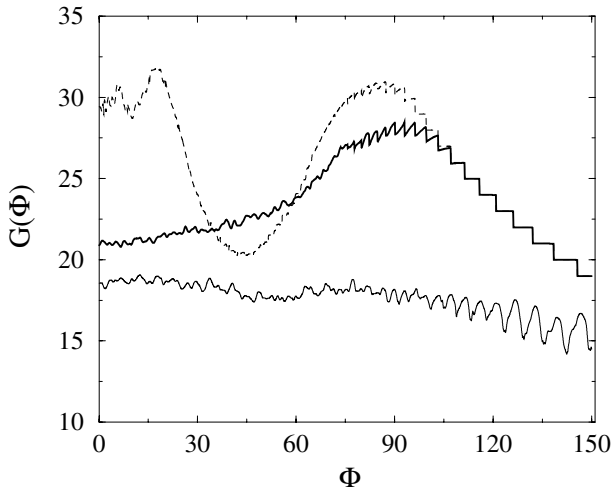

Figure 3. Magnetoconductance versus magnetic flux (both in units of their respective quanta), in 97×97 dots with leads of width $W = 57$ connected at opposite corners of the dot. The results correspond to dots with: (i) no disorder (broken line); (ii) Anderson impurities with $\Delta = 6$ (a single realization of disorder) placed either on all surface sites except those coinciding with the lead entrance sites (continuous line) or $2L$ impurities distributed randomly within the dot (thin continuous line).

disorder can, instead, scatter carriers between opposite sides of the cavity. The results shown in figure 3 illustrate the only difference that we have found up to now between cavities with surface impurities and with a number of bulk impurities proportional to L [17]. Apart from this difference, the two behave very similarly and in line with what one expects to be the behaviour of quantum chaotic cavities [3].

We have investigated how this steady increase of the magnetoconductance is affected by the width of the leads. In order to reduce fluctuations, which are particularly important at small W [16], we have averaged the conductance over disorder realizations (600 realizations were included in the calculations). The results for a cavity with rather narrow leads attached at the dots in three different ways are illustrated in figure 4. At small fluxes (typically below 1–2 flux quanta) the expected Lorentzian peak characteristic of chaotic cavities [3] is obtained (not clearly visible in the figure). At higher fluxes, a range over which the conductance behaves in a way that is strongly dependent on the lead configuration is observed. Beyond, the conductance increases linearly with a slope which takes very similar values in the three cases shown in the figure. The crossover to the linear behaviour occurs at a flux for which the radius of the classical cyclotron orbit r_c is roughly $L/2$. In our units (flux and conductance quanta $\Phi_0 = G_0 = 1$ and energy $\hbar^2/(2ma^2) = t = 1$, where t is the hopping integral), r_c is given by

$$r_c = \hbar v_F \frac{(L-1)^2}{4\pi} \frac{\Phi_0}{\Phi} \tag{8}$$

where the Fermi velocity is given by

$$\hbar v_F = \langle 2\sqrt{\sin^2 k_x + \sin^2 k_y} \rangle_{E_F}.$$

At the energy chosen here, $\hbar v(E) \approx 2.2$. Then the flux at which $r_c = L/2$ is, for the size of figure 4, $\Phi = 17\Phi_0$, which is very close to the flux at which the above-mentioned crossover occurs.

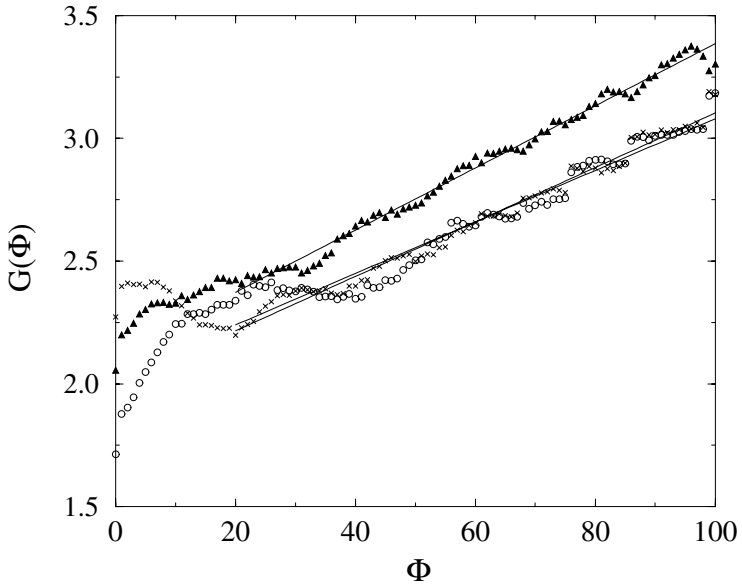

Figure 4. Magnetoconductance versus magnetic flux, in cavities of linear size $L = 47$ and leads of width 8 connected at: contiguous corners (circles), opposite corners (crosses), and one corner and the centre of the opposite side (triangles). Anderson impurities with $\Delta = 6$ were placed at all surface sites except those coinciding with the lead entrance sites. The results correspond to an energy $E = -\pi/3$ and an average over 600 disorder realizations. Straight lines were fitted for fluxes above 20. The fitted lines are: crosses: $G = 1.99 + 0.011\Phi$; circles: $G = 2.03 + 0.01\Phi$; and triangles: $G = 2.12 + 0.013\Phi$.

Figure 5 shows the averaged magnetoconductance for cavities of linear size $L = 47$ and lead widths in the range $W = 4$–20. It is noted that the linear behaviour discussed above appears in all cases at roughly the same magnetic flux, indicating that it is only related to the cavity size L, as suggested by the discussion above. Instead the slope increases with the width of the leads. At small W (systems with a low conductance) the conductance increases very slowly as a function of the magnetic flux. For sufficiently large W the conductance reaches a maximum and then decreases stepwise. As remarked above, the latter is a consequence of the overall depopulation of transverse modes (or Landau levels). The flux at which that maximum occurs decreases with W. In fact, it actually corresponds to $r_c \approx W/2$: introducing this value in equation (8) we obtain $\Phi_{\max} \approx 100$, 65, 50 and 40, to be compared with the numerical values of figure 5: 140, 90, 70 and 55, respectively. The agreement is reasonable. These results, combined with equation (8), indicate that $\Phi_{\max} \propto L^2/W$.

In figure 6 we plot the slope of the linear part of the magnetoconductance as a function of the width of the leads. The results can be accurately fitted by a W^2-law. The increase of the magnetoconductance can be understood in terms of the increase of the transmission probability of the transverse modes as their edge-like character increases and, consequently, its sensitivity to surface disorder is reduced. The steady increase in the conductance takes place until the above-mentioned depopulation begins to reduce the number of modes that participate in the current. Although this argument seems plausible, it cannot explain quantitative features of the results such as the linear relation between the conductance and the flux or the increase of the slope as the square of the lead width. This issue is addressed in the following section.

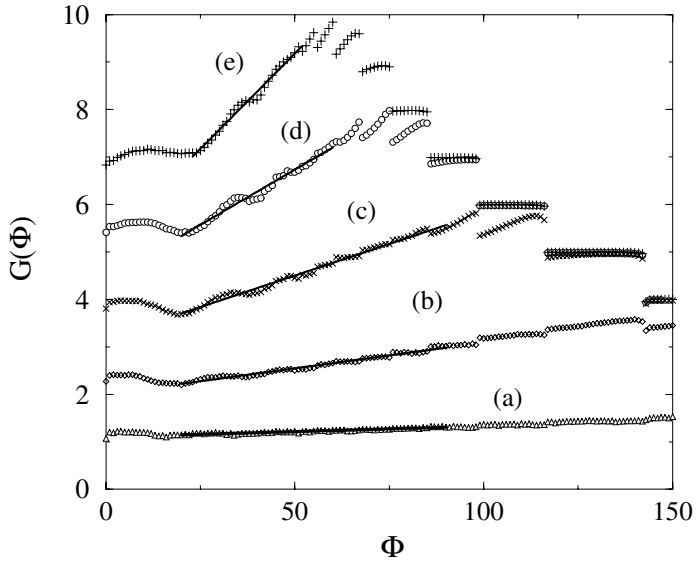

Figure 5. Magnetoconductance versus magnetic flux, in cavities of linear size $L = 47$ and leads of width $W = 4$ (a), 8 (b), 12 (c), 16 (d) and 20 (e), connected at opposite corners of the dot. Anderson impurities with $\Delta = 6$ were placed at all surface sites except those coinciding with the lead entrance sites. The results correspond to an energy $E = -\pi/3$ and an average over 600 disorder realizations. Straight lines were fitted for fluxes above 20 and below the flux at which the conductance shows a maximum. The slopes of the straight lines are plotted as a function of W^2 in figure 6.

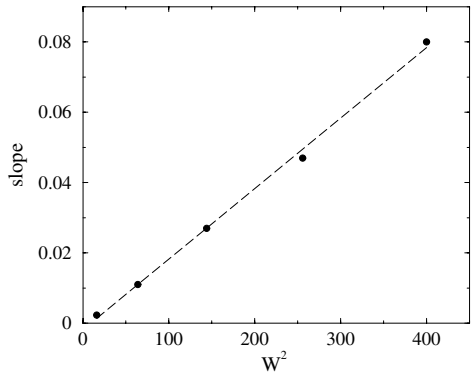

Figure 6. Slopes of the lines fitted in figure 5 versus the square of the width of the leads W. The fitted straight line is $-0.0019 + 2 \times 10^{-4} W^2$.

4. Discussion

The results discussed in the previous section resemble those predicted by Beenakker and van Houten for the magnetoconductance of two point contacts in series [10] and the related experiments of Staring *et al* [9]. Under the hypothesis that transmission between point contacts occurs with intervening equilibration of the current-carrying edge states, the authors of [10] derived the following expression for the conductance (in the following we take the conductance

and flux quanta $G_0 = \Phi_0 = 1$ and do not include spin degeneracy):

$$G(\Phi) = \left[\frac{1}{N_1} + \frac{1}{N_2} - \frac{1}{N_L}\right]^{-1} \tag{9}$$

where N_i are the number of occupied subbands in the two contacts or leads ($i = 1, 2$) and in the region between the contacts, or in the present case in the dot ($i = L$). Disregarding discreteness [10], N_i can be written as

$$N_i = \frac{n_i}{2B} f(\xi_i) \tag{10}$$

where n_i are the electron densities in the leads and in the region between them ($i = 1, 2$) and the function $f(\xi_i)$ is

$$f(\xi_i) = \begin{cases} \dfrac{2}{\pi}[\arcsin \xi_i + \xi_i(1 - \xi_i^2)^{1/2}] & \text{if } \xi_i < 1 \\ 1 & \text{if } \xi_i > 1 \end{cases} \tag{11}$$

with $\xi_i = l_i/2r_c$, l_i being a characteristic linear dimension in the three regions; in the present case, $l_i = W_1, W_2, L$.

We have used equations (9) and (10) to fit the numerical results of figure 5. We took as the fitting parameter the density or the Fermi velocity, $\hbar v_F = 2\sqrt{2\pi n}$, and assumed the same density in the leads and dot. As shown in figure 7, a satisfactory fitting is obtained for $\hbar v_F = 3.65$, almost twice the actual Fermi velocity in our model (see above). Note that one should not expect a better agreement, considering the important differences between the model used in the present numerical calculation and that of [10]. The theory reproduces the three regions that characterize our numerical results: an almost constant G for small flux or $r_c > L/2$, and a steadily increasing G up to $r_c \approx W/2$ followed by a steep decrease at higher fluxes. It is interesting to note that the theory of reference [10] shows a better agreement with the numerical results for the case in which the leads are attached at opposite corners of the dot than with those for the other two lead configurations of figure 4. A possible reason for this behaviour relies upon the equilibration assumption in Beenakker and van Houten theory. Equilibration is most likely when the leads are not facing each other, as is the case for leads attached to opposite

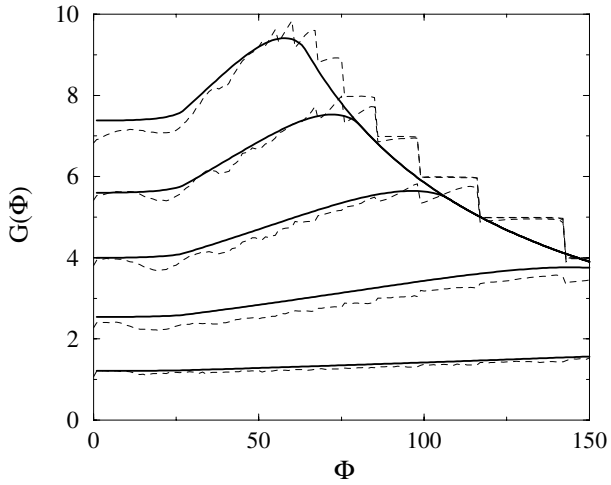

Figure 7. A fit of the numerical results of figure 5 by means of the theory of reference [10]—broken and continuous curves respectively (see the text).

corners. Instead, when leads are attached at contiguous corners, direct transmission is more probable and equilibration requires higher magnetic fields to take place. This is a figurative illustration of the assumptions under which the theory of reference [10] holds.

In order to check whether a linear relationship between the conductance and the flux over a rather wide range of fluxes, as indicated by the fits of figure 5, can be understood in terms of this theory, we have expanded the conductance for small ξ and $\xi_L > 1$. The result for leads having the same width and the same Fermi velocity (or density) in the leads and dot is

$$G(\Phi) \approx \frac{n_1}{2\pi B}\left[2\xi + \frac{4}{\pi}\xi^2 + \left(\frac{8}{\pi^2} - \frac{1}{3}\right)\xi^3\right]. \tag{12}$$

As the maximum in G occurs for ξ slightly smaller than unity, checking whether G varies linearly with the magnetic field below the maximum only requires one to calculate the ratio between the coefficients of the second and third powers of ξ in equation (12). This ratio is 2.82, indicating that the linear term dominates, in agreement with our numerical results. This equation also shows that the slope of the straight line is proportional to W^2. To make a quantitative comparison with the result of figure 6 we rewrite equation (12) introducing the actual expression for ξ; the result is

$$G(\Phi) \approx \frac{\hbar v}{4\pi}W + \frac{W^2}{\pi L^2}\Phi + \frac{\pi}{2\hbar v}\left(\frac{8}{\pi^2} - \frac{1}{3}\right)\frac{W^3}{L^2}\Phi^2. \tag{13}$$

The coefficient of the linear term turns out to be $1.44 \times 10^{-4} W^2$—not too far from the numerical result of figure 6.

5. Concluding remarks

Summarizing, we have presented a numerical analysis of the magnetoconductance of quantum chaotic cavities over a wide range of magnetic fields. For sufficiently open cavities the magnetoconductance increases steadily, reaching a maximum at a cyclotron radius $r_c \approx W/2$ (or, equivalently, a flux proportional to L^2/W). This steady increase of G agrees with the experimental observations reported in [4]. Neither regular nor bulk disordered cavities behave in this way. Numerical results for the average magnetoconductance indicate that, for magnetic fluxes larger than that for which the cyclotron radius is approximately $L/2$ and smaller than the flux at which the aforementioned maximum is reached, it increases linearly with the magnetic flux Φ with a slope proportional to the square of the width of the leads. At higher fluxes the conductance decreases stepwise. These results admit a satisfactory explanation in terms of the theory proposed by Beenakker and van Houten to interpret the experimental results for the magnetoconductance of two contacts in series. The fact that our results for small magnetic fluxes ($r_c > L/2$) show a better agreement with the theory in the case where the two contacts are attached to opposite corners of the dot (and, thus, are not facing each other) is related to the stronger equilibration of edge states promoted by this lead configuration with respect to the other two geometries explored in this work.

Acknowledgments

We thank C W J Beenakker and D Khmelnitskii for very useful correspondence, and L Brey, C Tejedor and J Palacios for interesting comments and remarks. This work was supported in part by the Spanish CICYT (grants PB96-0085 and 1FD97-1358).

References

[1] Marcus C M, Rimberg A J, Westervelt R M, Hopkins P F and Gossard A C 1992 *Phys. Rev. Lett.* **69** 506
Baranger H U, Jalabert R A and Stone A D 1993 *Phys. Rev. Lett.* **70** 3876
Chang A M, Baranger H U, Pfeiffer L N and West K W 1994 *Phys. Rev. Lett.* **73** 2111
Yang X, Ishio H and Burgdörfer J 1995 *Phys. Rev.* B **52** 8219

[2] Taylor R P, Newbury R, Sachrajda A S, Feng Y, Coleridge P T, Dettmann C, Zhu Ningjia, Guo Hong, Delage A, Kelly P J and Wasilewski Z 1997 *Phys. Rev. Lett.* **78** 1952

[3] Guhr T, Müller-Groeling A and Weidenmüller H A 1998 *Phys. Rep.* **299** 189

[4] Sachrajda A S, Ketzmerick R, Gould C, Feng Y, Kelly P J, Delage A and Wasilewski Z 1998 *Phys. Rev. Lett.* **80** 1948

[5] For reviews of mesoscopic physics see
Beenakker C W J and van Houten H 1991 *Solid State Physics* vol 44, ed H Ehrenreich and D Turnbull (New York: Academic) pp 1–228
Beenakker C W J and van Houten H 1991 *Mesoscopic Phenomena in Solids* ed B L Altshuler, P A Lee and R A Webb (New York: North-Holland)

[6] Datta S 1995 *Electronic Transport in Mesoscopic Systems* (Cambridge: Cambridge University Press)

[7] Altshuler B L, Aronov A G, Khmelnitskii D E and Larkin A I 1982 *Quantum Theory of Solids* ed I M Lifshits (Moscow: MIR)

[8] Beenakker C W J 1997 *Rev. Mod. Phys.* **69** 731

[9] Staring A A M, Molenkamp L W, Beenakker C W J, Kouwenhoven L P and Foxon C T 1990 *Phys. Rev.* **41** 8461

[10] Beenakker C W J and van Houten H 1989 *Phys. Rev.* **39** 10 445

[11] Cuevas E, Louis E and Vergés J A 1996 *Phys. Rev. Lett.* **77** 1970

[12] Louis E, Cuevas E, Vergés J A and Ortuño M 1997 *Phys. Rev.* B **56** 2120

[13] Blanter Y M, Mirlin A D and Muzykantskii B A 1998 *Phys. Rev. Lett.* **80** 4161
Tripathi V and Khmelnitskii D E 1998 *Phys. Rev.* B **58** 4161

[14] Vergés J A 1999 *Comput. Phys. Commun.* **118** 71

[15] Cuevas E, Louis E, Ortuño M and Vergés J A 1997 *Phys. Rev.* B **56** 15 853
Vergés J A, Cuevas E, Ortuño M and Louis E 1998 *Phys. Rev.* B **58** R10 143

[16] Louis E and Vergés J A 2000 *Phys. Rev.* B **61** 13 014

[17] Vergés J A and Louis E 1999 *Phys. Rev.* E **59** R3803